

ELASTIC: Efficient Once For All Iterative Search for Object Detection on Microcontrollers

Tony Tran, Qin Lin and Bin Hu

Abstract—Deploying high-performance object detectors on TinyML platforms poses significant challenges due to tight hardware constraints and the modular complexity of modern detection pipelines. Neural Architecture Search (NAS) offers a path toward automation, but existing methods either restrict optimization to individual modules—sacrificing cross-module synergy—or require global searches that are computationally intractable. We propose ELASTIC (Efficient Once for All Iterative Search for Object Detection on Microcontrollers), a unified, hardware-aware NAS framework that alternates optimization across modules (e.g., backbone, neck, and head) in a cyclic fashion. ELASTIC introduces a novel *Population Passthrough* mechanism in evolutionary search that retains high-quality candidates between search stages, yielding faster convergence, up to an 8% final mAP gain, and eliminates search instability observed without population passthrough. In a controlled comparison, empirical results show ELASTIC achieves +4.75% higher mAP and 2× faster convergence than progressive NAS strategies on SVHN, and delivers a +9.09% mAP improvement on PascalVOC given the same search budget. ELASTIC achieves 72.3% mAP on PascalVOC, outperforming MCUNET by 20.9% and TinyissimoYOLO by 16.3%. When deployed on MAX78000/MAX78002 microcontrollers, ELASTIC-derived models outperform Analog Devices’ TinySSD baselines, reducing energy by up to 71.6%, lowering latency by up to 2.4×, and improving mAP by up to 6.99 percentage points across multiple datasets. The experimental videos and codes are available on the project website¹.

Index Terms—Neural Architecture Search, TinyML, Object Detection, Population Passthrough, Iterative Evolutionary Architecture Search

I. INTRODUCTION

Object detection is a fundamental task in computer vision with real-world applications in mobile robotics, autonomous vehicles, smart surveillance, and embedded systems. While modern detectors achieve remarkable accuracy and speed on powerful hardware, their deployment on *TinyML platforms*—microcontrollers and edge devices with sub-MB memory, ultra-low power, and limited compute budgets—remains challenging [1], [2], [3], [4], [5].

Unlike image classification, object detection relies on a multi-stage pipeline—*backbone*, *neck* [6], and *head*—whose design choices are strongly interdependent: modifying one module changes the feature distributions and optimal configurations of the others. This cross-module coupling makes the detector design space highly combinatorial, which is particularly

challenging on microcontrollers where flash/SRAM budgets and inference cycles must be tightly controlled [7], [3], [8]. Recent hardware-aware NAS efforts for *pure MCU* targets have largely focused on *image classification* [9], [10], where the optimization is over single-stream networks with a single prediction head and classification objectives; in contrast, MCU detection requires jointly reasoning over the coupled backbone–neck–head pipeline and mAP-driven evaluation.

Recent TinyML-oriented detection research improves efficiency via specialized architectures and deployment-aware design. Hardware-conscious model and compilation/runtime co-design enable practical MCU execution [1], [8], [7], while lightweight detectors and variants (including transformer-inspired designs) explore accuracy–efficiency trade-offs under tight energy/latency constraints [3], [4], [5], [2]. Despite these advances, selecting an optimal detector for a specific MCU remains non-trivial because accuracy, flash/SRAM footprint, and inference cycles are tightly coupled, and manual design or ad-hoc scaling rarely navigates these constraints systematically at the full detector level.

Neural Architecture Search (NAS) offers a compelling approach to automate architecture design under tight resource constraints. Constraint-aware NAS has advanced edge classification [11], [1], [12], but object detection adds new layers of complexity. Prior detection NAS methods focus on individual modules (e.g., backbones [13], necks [6], or heads [14]), often ignoring cross-module dependencies. Full-pipeline NAS is possible [15], but scales poorly due to the massive combinatorial space—e.g., over 10^{28} configurations in realistic search settings [14], [16]. These observations expose a key gap: MCU-targeted detection NAS must preserve cross-module co-adaptation (backbone–neck–head interactions) without incurring the prohibitive cost of full end-to-end search, while enforcing hard resource constraints so discovered models are directly deployable.

To address these limitations, we introduce **ELASTIC** (Efficient Once for All Iterative Search for Object Detection on Microcontrollers), a novel once-for-all NAS method that performs *constrained iterative search*. ELASTIC alternates between optimizing one module while fixing others in a cyclic fashion, leveraging previous iteration feedback to refine architecture choices. This strategy preserves cross-module interdependencies while dramatically reducing the effective search space. Further, our approach enforces explicit resource constraints—such as model size—throughout the search process, ensuring deployability on MCUs.

Our key contributions are summarized as follows:

- **Unified Iterative NAS:** We propose a cyclic module-

T. Tran is with the Department of Research Computing, University of Houston, Houston, TX 77004 USA (e-mail: thtran37@CougarNet.UH.EDU).

Q. Lin, and B. Hu are with the Dept. of Electrical and Computer Engineering, and Dept. of Engineering Technology, University of Houston, Houston, TX 77004 USA (e-mail: qlin21@Central.UH.EDU, bhu11@Central.UH.EDU).

¹Project Website: <https://nail-uh.github.io/elastic.github.io/>

wise NAS framework that alternates optimization across the backbone, neck, and head to preserve cross-module co-adaptation while reducing search cost by restricting the active search dimension at each iteration. In our early-stage PascalVOC search, ELASTIC achieves up to **+4.75% mAP** over the progressive baseline while on SVHN, ELASTIC reduces search cost until convergence from **30.8 to 12.5 GPU hours**.

- **Population Passthrough Mechanism:** We introduce *Population Passthrough*, an elite-carryover strategy that stabilizes the *iterative* module alternation by retaining top-performing candidates when switching the active search module, rather than reinitializing the evolutionary population. This directly mitigates the abrupt performance drops observed under naive module switching and enables consistent convergence across iterations. On PascalVOC, enabling passthrough improves the final mAP from **22.1%** (iterative search *without* passthrough) to **30.83%** (with passthrough), demonstrating that the mechanism is a necessary component for making cyclic multi-module optimization effective in practice.
- **Enhanced Search Space:** ELASTIC enhances the search space over time. On SVHN, the mean mAP of randomly sampled architectures improves from **44.61% (joint)** to **70.68%** after 5 iterations, while variance reduces by **89.7%**. On PascalVOC, the mean mAP improves from **4.99%** to **28.32%**, with a **95.3% variance reduction**.
- **Once-for-All Deployment on Resource-Constrained Devices:** We validate ELASTIC in designing versatile models tailored to various resource constraints, demonstrating their inference efficiency on the MAX78000/02 and STM32F746 platform. Our ELASTIC model significantly outperforms the baseline [17] on the MAX78000 platform, achieving a **45.4% reduction** in energy consumption, a **29.3% decrease** in latency, and a **4.5% improvement** in mAP, demonstrating enhanced computational efficiency and accuracy.

II. RELATED WORK

NAS for Object Detection. Object detection architectures are modular, comprising a backbone, neck, and head. NAS methods have targeted these components individually or jointly: DetNAS [13] searches backbone architectures via a one-shot supernet; NAS-FPN [6] focuses on FPN design; NAS-FCOS [14] extends search to the FPN and head using reinforcement learning; MobileDets [18] introduces latency-aware backbone optimization for mobile accelerators; and Hit-Detector [15] jointly searches all modules but incurs high computational cost. While effective on larger systems, these methods are not designed for deployment on resource-constrained microcontrollers.

Progressive vs. Global Search. Global NAS jointly optimizes all modules but is intractable at TinyML scales due to the combinatorial size of the joint search space [15], [14]. Progressive NAS reduces complexity by optimizing modules sequentially—typically starting with the backbone or neck—while keeping previously optimized components

fixed [14], [19]. However, early architectural choices (e.g., output resolution, feature dimensionality, or stage depths) impose rigid interface constraints that limit the feasible design space for subsequent modules, often leading to suboptimal detection accuracy or violating tight memory and compute budgets in later stages [6]. Our approach addresses this by iteratively alternating module optimization, enabling cross-stage adaptation while preserving search efficiency.

OFA and Iterative NAS. Once-for-all (OFA) methods train a supernet capable of representing many sub-networks, enabling fast specialization to various hardware or latency constraints without retraining [11]. DetOFA [16] adapts this strategy to object detection using constraint-aware path pruning. These methods provide a foundation for efficient, hardware-aware NAS; our work builds on this by incorporating modular search dynamics specific to detection pipelines.

III. METHODOLOGY

This section introduces **ELASTIC**, a constrained iterative NAS method for *TinyML object detection* that explicitly treats the detector as a *multi-module pipeline* (backbone–neck–head). The key distinction from prior NAS strategies is that ELASTIC performs *cyclic module-wise optimization*: at each iteration, we optimize one module while keeping the others fixed, and we revisit modules multiple times to enable *cross-module co-adaptation* without incurring the prohibitive cost of full end-to-end search. However, naively switching the optimized module can destabilize the search and cause abrupt drops in validation performance. To address this, we propose **Population Passthrough**, which retains top-performing architecture candidates at the end of each module stage and injects them into the next stage, stabilizing convergence across iterations under explicit resource constraints.

A. Problem Formulation

Let an object detection subnet be represented as $\mathcal{N}(f, w)$ extracted from a supernet \mathcal{N} with architecture f and weights w . The search space \mathcal{A} contains all valid architectures such that $f \in \mathcal{A}$. The objective of NAS is to find the optimal architecture f^* that minimizes the validation loss \mathcal{L}_{val} when evaluated with shared weights W^* :

$$\min_{f \in \mathcal{A}} \mathcal{L}_{val}(\mathcal{N}(f, W^*(f))) \quad (1)$$

$$\text{s.t. } W^* = \arg \min_w \sum_{f \in \mathcal{A}} \mathcal{L}_{train}(\mathcal{N}(f, w)) \quad (2)$$

$$|W^*(f)| \leq \tau \quad (3)$$

Here, τ is the hardware-constrained model size. Inspired by Once-for-All NAS [11], a weight-shared supernet reduces training cost. Since \mathcal{A} grows combinatorially for joint optimization (e.g., $f = (b, h)$), optimization alternates between backbone b and head h . To extend this formulation to neck modules, the neck design choices can be integrated into the head search space, enabling joint optimization of both neck and head components within a single search stage.

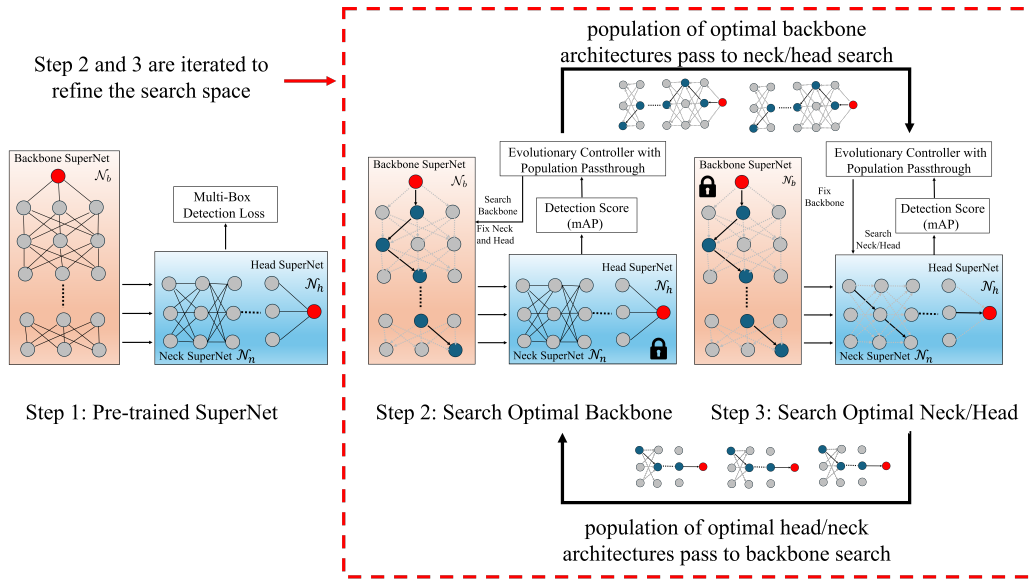


Fig. 1. **Overview of ELASTIC:** Our method begins with a pretrained supernet and performs iterative neural architecture search by alternating optimization between the backbone and head. The Population Passthrough mechanism ensures continuity by retaining top-performing candidates across module alternations.

At iteration t , we first optimize the backbone while keeping $h^{(t)}$ fixed:

$$b^{(t+1)} = \arg \min_b \mathcal{L}_{\text{val}}(\mathcal{N}((b, h^{(t)}), w^*)) \quad (4)$$

$$\text{s.t. } w^* = \arg \min_w \sum_{f \in \mathcal{A}} \mathcal{L}_{\text{train}}(\mathcal{N}(f, w)) \quad (5)$$

$$|w_b| \leq \tau_b \quad (6)$$

Then, we fix $b^{(t+1)}$ and update the head:

$$h^{(t+1)} = \arg \min_h \mathcal{L}_{\text{val}}(\mathcal{N}((b^{(t+1)}, h), w^*)) \quad (7)$$

$$\text{s.t. } w^* = \arg \min_w \sum_{f \in \mathcal{A}} \mathcal{L}_{\text{train}}(\mathcal{N}(f, w)) \quad (8)$$

$$|w_h| \leq \tau_h \quad (9)$$

We enforce the constraint $\tau_b + \tau_h \leq \tau$, where τ is the global memory budget. This formulation ensures that each module’s optimization phase respects deployment constraints.

B. Iterative Evolutionary Architecture Search

At the core of ELASTIC is an *Iterative Evolutionary Architecture Search* that alternates optimization between the backbone and the head over successive cycles. As illustrated in Fig. 1, the framework does not search the full detector space in a single pass. Instead, it fixes one module while optimizing the other, then switches roles and repeats this process iteratively. This design preserves search tractability for TinyML deployment while allowing the two modules to progressively co-adapt across iterations.

Within each stage shown in Fig. 1, the evolutionary search follows a standard population-based procedure, but is applied only to the currently active module. The population is initialized using two sources: high-performing candidates carried

over from the module’s previous visit through *Population Passthrough*, and newly sampled candidates that maintain exploration. New architectures are then generated through crossover and mutation under the corresponding resource constraints (e.g., τ_b for the backbone and τ_h for the head). Each candidate is evaluated inside the weight-shared supernet using validation mAP, where the complementary module remains fixed. The best-performing candidates are retained to guide the next generation and to provide a strong starting point when the search returns to that module in a later cycle.

As depicted in Fig. 1, once the search for the current module is completed, ELASTIC switches to the other module and repeats the same procedure. By alternating in this back-and-forth manner, the framework incrementally refines both modules rather than optimizing them only once. This repeated revisiting is important because improving one module changes the context in which the other operates. Therefore, the iterative structure of ELASTIC enables the backbone and head to adapt to each other over time while remaining within deployment constraints.

C. Population Passthrough

A key practical challenge in ELASTIC’s *outer-loop* cyclic module-wise optimization is maintaining optimization continuity when switching the *active* module (e.g., backbone \rightarrow neck/head \rightarrow backbone). Although the *inner-loop* evolutionary optimizer is standard, naive alternation effectively *cold-starts* each stage by discarding the module-specialized population, forcing repeated re-discovery of candidates compatible with the fixed context.

To make alternation workable, we introduce **Population Passthrough**, a lightweight memory mechanism that transfers elite architectural “knowledge” across module switches. For each module $m \in \{b, h\}$ (backbone vs. neck/head), we maintain a *passthrough buffer* \mathcal{M}_m containing the top-performing candidates (ranked by validation mAP under the

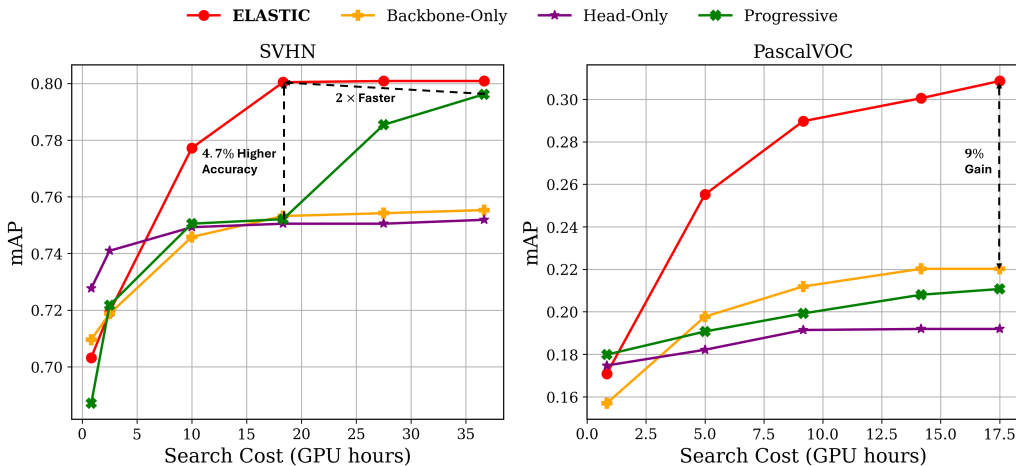


Fig. 2. Comparison of Neural Architecture Search (NAS) strategies on the SVHN (left) and PascalVOC (right) subset. On the SVHN dataset, ELASTIC achieves 4.7% higher mAP and 2× faster than Progressive. On PascalVOC, ELASTIC achieves a 9% absolute mAP gain over all other approaches in 17.5 GPU hours.

TABLE I
QUANTITATIVE COMPARISON OF SEARCH STRATEGIES ON THE SVHN AND PASCALVOC SUBSET. ELASTIC CONSISTENTLY ACHIEVES THE HIGHEST mAP ON BOTH DATASETS AND REDUCES GPU HOURS BY 59% ON SVHN.

Dataset	Method	mAP	↑mAP	Cost	MACs	Params	Latency
SVHN	Backbone-Only [13], [20], [21]	75.53%	+0.18%	10.8 hrs	137.6 M	0.73 M	2.62 ms
	Neck/Head-Only [6], [22], [23]	75.35%	+0.00%	4.7 hrs	475.3 M	1.01 M	2.69 ms
	Progressive [14]	79.62%	+4.27%	30.8 hrs	78.4 M	0.52 M	2.36 ms
	ELASTIC (OURS)	80.09%	+4.74%	12.5 hrs	105.8 M	0.61 M	2.34 ms
PascalVOC	Backbone-Only [13]	22.02%	+2.80%	9.6 hrs	436.1 M	0.58 M	2.11 ms
	Neck/Head-Only [6], [22], [23]	19.22%	+0.00%	6.0 hrs	240.0 M	0.36 M	2.48 ms
	Progressive [14]	21.74%	+2.52%	14.8 hrs	540.0 M	0.41 M	2.66 ms
	ELASTIC (OURS)	30.83%	+11.61%	14.65 hrs	642.8 M	0.57 M	2.00 ms

current resource constraints) from the most recent optimization of m . When ELASTIC revisits m , we initialize the population by mixing a fixed fraction of elites from \mathcal{M}_m (inheritance) with newly sampled/mutated candidates (diversity), balancing exploitation and exploration.

This mechanism is *new in our setting* because it targets *alternating modular NAS*: unlike standard elitism/aging schemes that assume a single, fixed search space and continuous run, Population Passthrough is applied *at module boundaries* to stabilize the outer-loop alternation and avoid repeated re-discovery.

D. Resource Allocation and Search Budget

To ensure deployability on resource-constrained hardware, we explicitly partition the overall memory budget τ between architectural modules. Let τ_b and τ_h denote the memory allocations for the backbone and head, respectively, such that $\tau_b + \tau_h \leq \tau$. This modular budget decomposition is critical for embedded systems, where hardware constraints—such as on-chip SRAM, flash storage, and runtime latency—are rigid and non-negotiable [4]. By enforcing per-module constraints during search, ELASTIC ensures that all discovered subnetworks are compatible with the deployment requirements of target TinyML platforms.

In addition, ELASTIC is designed to support *search interruption*, allowing the iterative process to be paused at any stage and a valid, high-quality subnetwork to be extracted. This property is particularly beneficial in real-world TinyML development workflows, where compute resources are limited and iterative refinement may need to occur incrementally [2].

IV. EXPERIMENTS

A. Experimental Setup

We construct five OFA-based supernet architectures tailored for diverse TinyML-relevant datasets: (i) *SVHN*, (ii) *VGGFace2*, (iii) a five-class subset of *PascalVOC*, (iv) the full *PascalVOC* dataset, and (v) *TrashNet*. These datasets are selected to cover a range of TinyML application domains, from lightweight digit recognition to face identification and general-purpose object detection, while avoiding the prohibitive memory and compute demands of large-scale datasets such as COCO.

The *SVHN*, *VGGFace2*, and *PascalVOC subset* supernet architectures adopt a one-stage SSD-style architecture, while the *full PascalVOC* and *TrashNet* supernet architectures adopt a MobileNet–YOLO style design that combines a lightweight MobileNet backbone with YOLO-style detection heads. For the SSD-style supernet architectures, the search space varies (i) layer widths, (ii) kernel sizes (1×1 , 3×3), and (iii) depth, i.e., the number of layers allocated at

TABLE II

COMPARISON OF ELASTIC WITH TINYSSIMOYOLO [24] AND MCUNET [1], [25] ON THE FULL PASCALVOC DATASET, CONSIDERING ALL OBJECT CLASSES AND COUNTS. ELASTIC ACHIEVES A 20.9% mAP BOOST OVER MCUNET [1], 4.0% OVER MCUNETV2 [25], AND A 16.3% OVER TINYSSIMOYOLO’S [24] BEST PERFORMING MODEL, WHILE DISCOVERING A MODEL WITH SIGNIFICANTLY FEWER MACS, ENABLING FASTER INFERENCE.

Method	MACs	↓MACs	Params	VOC mAP	↑mAP
TY: 20-3-88 [24]	32M	90.7%	0.58M	53%	+30%
TY: 20-7-88 [24]	44M	87.2%	0.58M	47%	+24%
TY: 20-3-112 [24]	54M	84.3%	0.89M	56%	+33%
TY: 20-7-112 [24]	70M	79.6%	0.91M	53%	+30%
TY: 20-3-224 [24]	218M	36.4%	3.34M	23%	+0%
MCUNet [1]	168M	51.0%	1.2M	51.4%	+28.4%
MCUNetV2-M4 [25]	172M	49.9%	0.47M	64.6%	+41.6%
MCUNetV2-H7 [25]	343M	0%	0.67M	68.3%	+45.3%
ELASTIC (OURS)	86M	74.9%	1.36M	72.3%	+49.3%

TABLE III

MEAN mAP AND VARIANCE ACROSS SEARCH SPACES. SUPERSCRIPTS DENOTE ITERATIVE SEARCH ITERATIONS. HIGHER MEAN mAP IS BETTER; LOWER VARIANCE INDICATES MORE CONSISTENT ARCHITECTURES.

Dataset	Search Space	Mean mAP	↑mAP	Std. Dev.	Variance
SVHN	Joint Search [15]	44.61%	0%	1.39	1.93
	Neck/Head Search [6], [22], [23]	67.38%	+22.77%	0.37	0.136
	ELASTIC ⁽³⁾	70.42%	+25.81%	0.47	0.221
	ELASTIC ⁽⁵⁾	70.68%	+26.07%	0.45	0.199
PascalVOC	Joint Search [15]	4.99%	0%	0.04	1.40×10^{-3}
	Neck/Head Search [6], [22], [23]	27.89%	+22.90%	0.01	9.86×10^{-5}
	ELASTIC ⁽³⁾	28.28%	+23.29%	0.01	7.04×10^{-5}
	ELASTIC ⁽⁵⁾	28.32%	+23.33%	0.01	6.60×10^{-5}

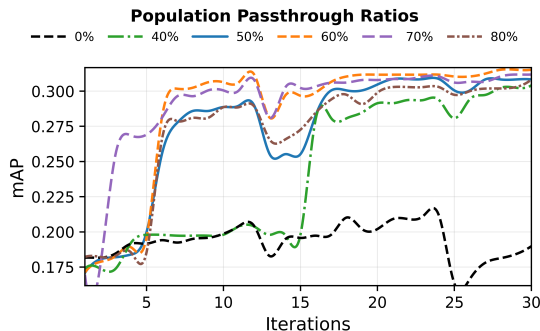


Fig. 3. **Effect of Population Passthrough on Search Stability.** Eliminating passthrough (0%) leads to unstable search dynamics, with mAP repeatedly dropping and stalling at 22.1%. Introducing a moderate passthrough rate (50–80%) stabilizes training and improves convergence, achieving over 30% mAP (+8%).

each feature map. For both the MobileNet–YOLO supernet, the search space varies (i) expansion ratios, (ii) kernel sizes (1×1 , 3×3), and (iii) depth, i.e., the number of blocks allocated at each feature map.

All supernet are trained with a batch size of 64, learning rate of 0.001, momentum of 0.9, and weight decay of 5×10^{-4} . Training follows the progressive shrinking strategy [11], with 200 epochs per level transition. Experiments are conducted on a single NVIDIA RTX 4090 GPU.

We evaluate deployment across three MCU platforms. The MAX78000/02 are accelerator-equipped microcontrollers

with a dedicated CNN engine and separate on-chip memory for weights and activations. MAX78000 provides 442 kB weight memory and 524 kB data memory for the earliest streaming layers, while subsequent layers must fit within a single 32 kB memory instance. MAX78002 provides 2.4 MB weight memory and 1.3 MB data memory for the earliest streaming layers, while subsequent layers must fit within a single 80 kB memory instance. In contrast, the STM32F746 is a general-purpose microcontroller without a CNN accelerator, with 320 kB SRAM and 1 MB flash, where weights are stored in flash and activations are stored in SRAM. In this way, MAX78000/MAX78002 represent accelerator-equipped TinyML targets, while STM32F746 provides a non-accelerator MCU baseline for comparison.

Evolutionary search is performed with a population size of 100, mutation probability of 0.2, mutation ratio of 0.5, and a parent selection ratio of 0.25. Each search is budgeted for 55 generations on SVHN and VGGFace2, and 30 generations on the PascalVOC subset, full PascalVOC, and TrashNet datasets, respectively. Convergence is defined as the point at which the best candidate architecture’s mAP is within 1% of the final value achieved at the end of the search.

B. Comparative Search Evaluation

We evaluate the effectiveness of **ELASTIC** by comparing it against three baseline NAS strategies: *backbone-only search* [13], *head-only search* [14], and *progressive NAS* [14].

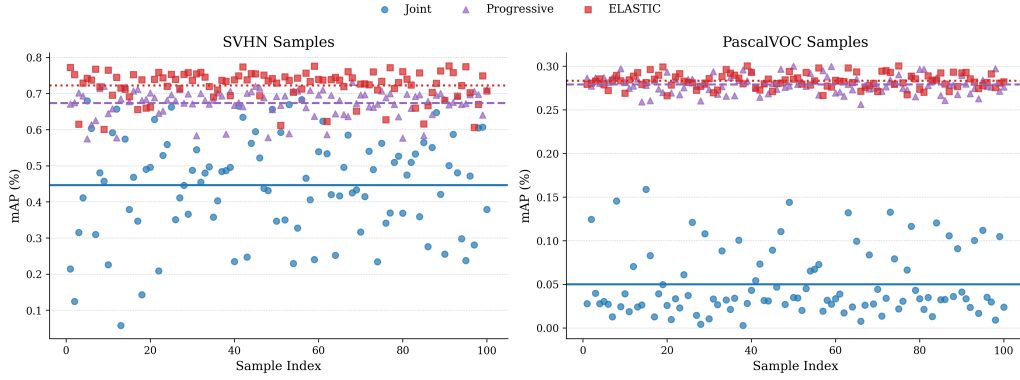


Fig. 4. **Search space refinement through ELASTIC iteration.** Distributions of 100 randomly sampled architectures from three head search spaces—joint NAS, progressive head-only, and ELASTIC-refined—on SVHN (left) and PascalVOC (right). ELASTIC produces architectures with a mean mAP improvement of +4.87% on SVHN and +0.43% on PascalVOC over progressive search. Compared to global joint search, ELASTIC improves the mAP by 26.07% and 23.33% on SVHN and PascalVOC, respectively.

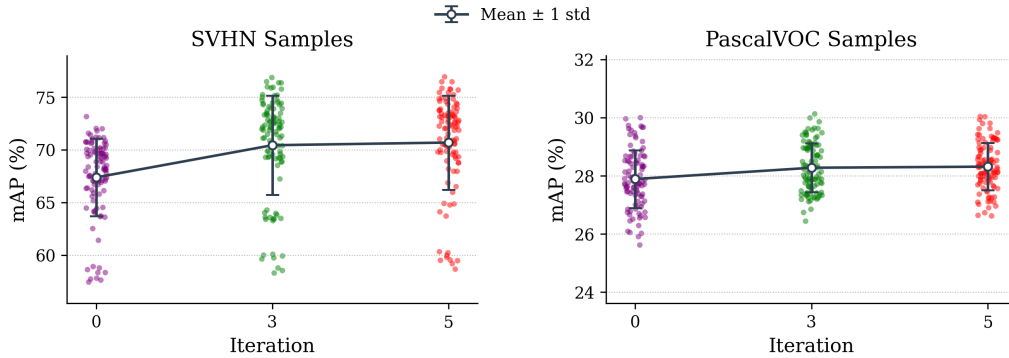


Fig. 5. **Search Space Evolution Over Iterations.** Mean accuracy and distribution of sampled architectures at iterations 0, 3, and 5. On SVHN, mean mAP improves by 3.3% and variance drops by 89.7%; on PascalVOC, mean mAP rises from 27.89% to 28.32% and variance decreases by 33%.

All methods are evaluated under a fixed budget using a consistent once-for-all supernet design.

a) Results on SVHN and PascalVOC subset.: Table I summarizes our search results. On SVHN, ELASTIC achieves a final mAP of **80.09%**, outperforming progressive NAS (79.62%) while using only 12.5 GPU hours—a **2 \times speedup** compared to the 30.8 hours required by progressive search. On PascalVOC, the improvement is more substantial: ELASTIC reaches **30.83% mAP**, outperforming progressive NAS (**21.74%**) by **+9.09 percentage points** with similar compute (14.65 vs. 14.78 GPU hours).

b) Effect of Decoupling.: To isolate the impact of coordinated multi-module optimization, we compare ELASTIC against decoupled strategies that search only the backbone or the head. On SVHN, these methods achieve significantly lower performance: backbone-only search yields **75.53% mAP** and head-only search reaches just **75.35%**, falling short of ELASTIC’s **80.09%** by **4.75 percentage points**.

c) Convergence Behavior.: Figure 2 shows that ELASTIC converges up to **2 \times faster** than progressive NAS. On SVHN, ELASTIC converges in just **15 iterations**, compared to **over 30 iterations** for progressive NAS. In contrast, backbone-only and head-only searches stagnate early, **plateauing at 75.53% and 75.35% mAP**, respectively. A similar trend holds on

PascalVOC, where ELASTIC rapidly reaches **30.83% mAP**, outperforming progressive NAS (**21.74%**) and single-module baselines (**22.02%** and **19.22%**). This disparity is exacerbated by progressive NAS’s rigid search pipeline, which fixes early module choices and prevents adaptation to downstream module configurations.

d) Comparison with MCUNET and TinyissimoYOLO.: To assess ELASTIC’s suitability for microcontrollers, we extend our experiments using the MCUNET [1] search space with the neck module included for fair comparison. Benchmarked on the full PascalVOC (224 \times 224) dataset with similar parameter budgets (Table II), our ELASTIC-derived detector achieves **72.3% mAP**, surpassing MCUNET by **20.9%**, TinyissimoYOLO’s [3] best model by **16.3%**, and MCUNetV2-M4/H7 [25] by **7.7%** and **4.0%**, respectively, while using **50–75% fewer MACs**. Unlike MCUNetV2 [25], which requires external patch-based inference, ELASTIC supports native end-to-end inference, making it easier to deploy across diverse microcontrollers.

C. Impact of Population Passthrough on Search Stability

Iterative NAS can suffer sharp drops at module boundaries because switching the active module effectively resets the evolutionary population. Without population memory, each alternation incurs a repeated “catch-up” phase to re-discover

TABLE IV

ACCURACY AND EFFICIENCY ACROSS DATASETS AND MCUs. WE REPORT PARAMETER COUNT, DETECTION ACCURACY, AND PER-INFERENCE EFFICIENCY FOR MODELS ON MAX78000/02 AND STM32F746. ENERGY AND POWER ARE OMITTED FOR STM32F746 DUE TO SETUP LIMITATIONS. NOTE WE SCALE MODELS DEPLOYED ON THE MAX78002, PRESERVING KEY ARCHITECTURAL CHOICES, TO DEPLOY FOR COMPARISON ON THE STM32F746.

Model	Dataset	Device	Params	Energy (μJ)	Latency (ms)	Power (mW)	mAP (%)
ai87-fpndetector [17]	PascalVOC	MAX78002	2.18M	62001	122.6	445.76	50.66
ELASTIC (OURS)	PascalVOC	MAX78002	1.32M	17581	51.1	285.02	57.65
ai87-fpndetector [17]	PascalVOC	STM32746	0.82M	N/A	494.8	N/A	9.12
ELASTIC (OURS)	PascalVOC	STM32746	0.89M	N/A	490.6	N/A	19.0
ai87-fpndetector [17]	TrashNet	MAX78002	2.18M	62001	122.6	445.76	83.1
ELASTIC (OURS)	TrashNet	MAX78002	1.32M	17581	51.1	285.02	93.3
ai87-fpndetector [17]	TrashNet	STM32746	0.82M	N/A	494.8	N/A	54.03
ELASTIC (OURS)	TrashNet	STM32746	0.89M	N/A	490.6	N/A	73.9
ai85net-tinierSSD-face [17]	VGGFace2	MAX78000	0.28M	1712	43.4	29.90	84.72
ELASTIC (OURS)	VGGFace2	MAX78000	0.22M	1368	45.6	20.90	87.10
ai85net-tinierSSD-face [17]	VGGFace2	STM32746	0.277M	N/A	968.2	N/A	80.2
ELASTIC (OURS)	VGGFace2	STM32746	0.168M	N/A	699.1	N/A	82.1
ai85net-tinierSSD [17]	SVHN	MAX78000	0.19M	573	14.0	29.20	83.60
ELASTIC (OURS)	SVHN	MAX78000	0.22M	341	13.0	16.70	88.10
ai85net-tinierSSD [17]	SVHN	STM32746	0.229M	N/A	449.3	N/A	83.5
ELASTIC (OURS)	SVHN	STM32746	0.235M	N/A	523.7	N/A	87.9

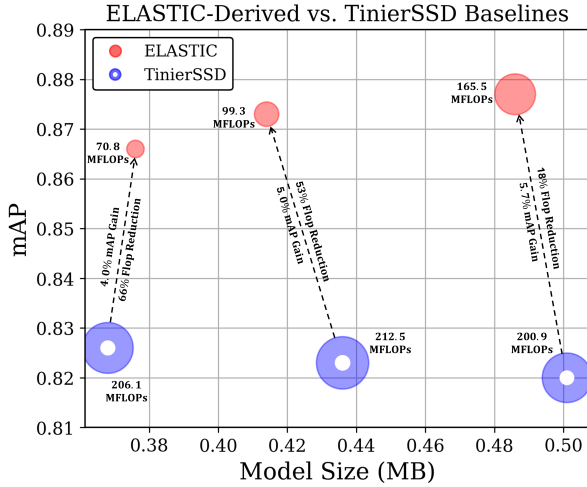


Fig. 6. Comparison of ELASTIC-derived models vs. scaled ai85net-tinierSSD [17] baselines. Marker size reflects number of FLOPs, positively correlated with energy. ELASTIC-derived models can reduce FLOPs by up to 66% with up to a 5.7% accuracy gain.

compatible high-quality candidates, harming stability and slowing convergence. We mitigate this with *Population Passthrough*, which carries a fixed fraction of elite architectures into the next stage to preserve optimization momentum.

Figure 3 ablates the passthrough ratio on PascalVOC. With **0%** passthrough, mAP collapses after switches and **saturates below 22%**. Ratios of **50–80%** stabilize the search and reach **> 30%** mAP in roughly half the iterations. **60%** performs best, balancing exploitation (stability) and exploration (progress).

D. Iterative Search Space Refinement

To evaluate whether ELASTIC improves the *effective* search space, we randomly sample 100 architectures from three *matched* spaces: (1) *joint* backbone–neck/head, (2) *progressive* head-only (fixed backbone), and (3) *ELASTIC-refined* head-only (after re-optimization) in Figure 4. On SVHN, the mean mAP increases from **44.61%** (joint) to **67.38%** (progressive) and to **72.25%** with ELASTIC (**+4.87%** vs. progressive). On PascalVOC, the mean improves from **4.99%** (joint) to **27.89%** (progressive) and to **28.32%** with ELASTIC.

We further track refinement over iterations by repeating the sampling at iterations **0, 3, 5** (Fig. 5, Table III), treating iteration **0** as the progressive baseline. On SVHN, the mean mAP rises from **67.38%** (iter. 0) to **70.68%** (iter. 5), with variance changing from **0.136** to **0.199**. On PascalVOC, the mean increases from **27.89%** to **28.32%**, while variance decreases from 9.86×10^{-5} to 6.60×10^{-5} . Overall, iterative revisiting yields a stronger induced space than progressive partitioning and improves stability on PascalVOC.

E. Deployment on MCU Platforms

The MAX78000/MAX78002 MCUs integrate a CNN accelerator but impose tight constraints on kernel sizes, layer counts, and memory. Despite these limits, ELASTIC-derived models improve the efficiency–accuracy trade-off over TinierSSD/FPN baselines [17] while remaining within on-chip budgets.

We highlight these results in Table IV. On PascalVOC, energy decreases by **71.6%**, latency by **2.40 \times** , power by **36.1%**, and mAP increases by **+6.99** on MAX78002. On TrashNet, ELASTIC follows the same pattern on MAX78002: energy decreases by **71.6%**, latency by **2.40 \times** , power by **36.1%**, and mAP increases by **+10.2**. ELASTIC also generalizes across tasks: on VGGFace2, it reduces energy and power by **20.1%**

TABLE V

ACCURACY COMPARISON ON STM32F746 AT MULTIPLE INPUT RESOLUTIONS. NOTE WE SCALE THESE MODELS DOWN, PRESERVING KEY ARCHITECTURAL CHOICES, TO DEPLOY ON THE STM32F746. THE MAXIMUM INPUT RESOLUTION AI87-FPNDETECTOR CAN DEPLOY ON IS (100×100) WHILE ELASTIC IS (128×128) .

Model	Dataset	Device	Params	Resolution	Latency (ms)	mAP (%)
ai87-fpndetector [17]	PascalVOC	STM32746	0.82M	128×128	N/A	OOM
ai87-fpndetector [17]	PascalVOC	STM32746	0.82M	100×100	494.8	9.12
ELASTIC (OURS)	PascalVOC	STM32746	0.89M	128×128	825.55	40.1
ELASTIC (OURS)	PascalVOC	STM32746	0.89M	100×100	490.6	19.0
ai87-fpndetector [17]	TrashNet	STM32746	0.82M	128×128	N/A	OOM
ai87-fpndetector [17]	TrashNet	STM32746	0.82M	100×100	494.8	54.03
ELASTIC (OURS)	TrashNet	STM32746	0.89M	128×128	825.55	86.0
ELASTIC (OURS)	TrashNet	STM32746	0.89M	100×100	490.6	73.9

and **30.1%**, respectively, while improving mAP by **+2.38**; on SVHN, it reduces energy and power by **40.5%** and **42.8%**, respectively, with a **+4.50** mAP gain and a slight latency improvement. We further evaluate cross-device portability on STM32F746. On PascalVOC, the scaled ELASTIC model reduces latency slightly from **494.8 ms** to **490.6 ms** while improving mAP from **9.12** to **19.0**. On TrashNet, the scaled ELASTIC model reduces latency slightly from **494.8 ms** to **490.6 ms** while improving mAP from **54.03** to **73.9**. On VGGFace2, ELASTIC reduces latency by **27.8%** and improves mAP by **+1.9**. On SVHN, ELASTIC improves mAP by **+4.4**.

Since the two scaled STM32F746 models differ in their maximum deployable input resolution, we also compare them at both 100×100 and 128×128 in Table V. The scaled ai87-fpndetector baseline can be deployed only up to 100×100 , while the scaled **ELASTIC** model remains deployable at 128×128 ; at 128×128 , the baseline encounters out-of-memory due to activation SRAM limits on STM32F746. Under matched 100×100 resolution, ELASTIC still outperforms the baseline on both datasets, improving mAP from **9.12** to **19.0** on PascalVOC and from **54.03** to **73.9** on TrashNet, while maintaining nearly identical latency (**490.6 ms** vs. **494.8 ms**). Moreover, ELASTIC supports the higher 128×128 resolution and achieves **40.1** mAP on PascalVOC and **86.0** mAP on TrashNet, further highlighting that the searched architecture is not only more accurate but also more deployable under tight STM32F746 memory constraints.

Figure 6 compares ELASTIC architectures to scaled TinierSSD baselines [17] and shows ELASTIC attains higher accuracy at lower compute (**66%** FLOPs reduction), underscoring the value of hardware-aware NAS for MCU deployment.

V. CONCLUSION

We introduced **ELASTIC**, a unified framework for constrained, once-for-all NAS tailored to object detection on resource-limited platforms. By alternating backbone and head optimization, ELASTIC enables cross-module co-adaptation while significantly reducing search cost. A key component of our approach, *Population Passthrough*, stabilizes module transitions and accelerates convergence, addressing a major limitation of existing progressive and decoupled NAS methods.

Through extensive experiments on multiple datasets and deployment on real microcontroller platforms, we demonstrated



Fig. 7. **ELASTIC** deployment on MAX78000 using SVHN dataset. ELASTIC produces compact, high-performing architectures suitable for ultra-low-power deployment.

that ELASTIC discovers architectures that are more accurate and more efficient than manually designed and standard NAS baselines. These results highlight the effectiveness of iterative, hardware-aware NAS in advancing the accuracy–efficiency frontier for resource-constrained edge devices.

REFERENCES

- [1] J. Lin, W.-M. Chen, Y. Lin, j. cohn, C. Gan, and S. Han, “MCUNet: Tiny Deep Learning on IoT Devices,” in *Advances in Neural Information Processing Systems*, vol. 33. Curran Associates, Inc., 2020, pp. 11 711–11 722. [Online]. Available: https://proceedings.neurips.cc/paper_files/paper/2020/hash/86c51678350f656dcc7f490a43946ee5-Abstract.html
- [2] Y. Liang, Z. Wang, X. Xu, Y. Tang, J. Zhou, and J. Lu, “MCUFormer: Deploying Vision Transformers on Microcontrollers with Limited Memory,” Dec. 2023, arXiv:2310.16898 [cs]. [Online]. Available: <http://arxiv.org/abs/2310.16898>
- [3] J. Moosmann, M. Giordano, C. Vogt, and M. Magno, “TinyissimoYOLO: A Quantized, Low-Memory Footprint, TinyML Object Detection Network for Low Power Microcontrollers,” in *2023 IEEE 5th International Conference on Artificial Intelligence Circuits and Systems (AICAS)*, Jun. 2023, pp. 1–5, arXiv:2306.00001 [cs, eess]. [Online]. Available: <http://arxiv.org/abs/2306.00001>
- [4] A. Moss, H. Lee, L. Xun, C. Min, F. Kawsar, and A. Montanari, “Ultra-Low Power DNN Accelerators for IoT: Resource Characterization of the MAX78000,” in *Proceedings of the 20th ACM Conference on Embedded Networked Sensor Systems*. Boston Massachusetts: ACM, Nov. 2022, pp. 934–940. [Online]. Available: <https://dl.acm.org/doi/10.1145/3560905.3568300>
- [5] B. Yan, H. Peng, K. Wu, D. Wang, J. Fu, and H. Lu, “LightTrack: Finding Lightweight Neural Networks for Object Tracking via One-Shot Architecture Search,” Apr. 2021, arXiv:2104.14545 [cs]. [Online]. Available: <http://arxiv.org/abs/2104.14545>

- [6] G. Ghiasi, T.-Y. Lin, R. Pang, and Q. V. Le, "NAS-FPN: Learning Scalable Feature Pyramid Architecture for Object Detection," Apr. 2019, arXiv:1904.07392 [cs]. [Online]. Available: <http://arxiv.org/abs/1904.07392>
- [7] G. Wang, Z. P. Bhat, Z. Jiang, Y.-W. Chen, D. Zha, A. C. Reyes, A. Niktash, G. Ulkar, E. Okman, X. Cai, and X. Hu, "BED: A Real-Time Object Detection System for Edge Devices," Sep. 2022, arXiv:2202.07503 [cs]. [Online]. Available: <http://arxiv.org/abs/2202.07503>
- [8] A. Burrello, A. Garofalo, N. Bruschi, G. Tagliavini, D. Rossi, and F. Conti, "DORY: Automatic End-to-End Deployment of Real-World DNNs on Low-Cost IoT MCUs," *IEEE Transactions on Computers*, vol. 70, no. 8, pp. 1253–1268, Aug. 2021. [Online]. Available: <https://ieeexplore.ieee.org/document/9381618/>
- [9] A. M. Garavagno, E. Ragusa, A. Frisoli, and P. Galstalo, "An affordable hardware-aware neural architecture search for deploying convolutional neural networks on ultra-low-power computing platforms," *IEEE Sensors Letters*, vol. 8, no. 5, pp. 1–4, May 2024.
- [10] —, "Searching neural architectures for sensor nodes on iot gateways," *IEEE Internet of Things Journal*, vol. 12, no. 21, pp. 1–1, Nov. 2025.
- [11] H. Cai, C. Gan, T. Wang, Z. Zhang, and S. Han, "Once-for-All: Train One Network and Specialize it for Efficient Deployment," Apr. 2020, arXiv:1908.09791 [cs, stat]. [Online]. Available: <http://arxiv.org/abs/1908.09791>
- [12] H. Lv, L. Zhang, and Y. Wang, "In-Situ NAS: A Plug-and-Search Neural Architecture Search Framework Across Hardware Platforms," *IEEE Transactions on Computers*, vol. 74, no. 9, pp. 2856–2869, Sep. 2025. [Online]. Available: <https://ieeexplore.ieee.org/document/11003207/>
- [13] Y. Chen, T. Yang, X. Zhang, G. Meng, X. Xiao, and J. Sun, "DetNAS: Backbone Search for Object Detection," Dec. 2019, arXiv:1903.10979 [cs]. [Online]. Available: <http://arxiv.org/abs/1903.10979>
- [14] N. Wang, Y. Gao, H. Chen, P. Wang, Z. Tian, C. Shen, and Y. Zhang, "NAS-FCOS: Fast Neural Architecture Search for Object Detection," Feb. 2020, arXiv:1906.04423 [cs]. [Online]. Available: <http://arxiv.org/abs/1906.04423>
- [15] J. Guo, K. Han, Y. Wang, C. Zhang, Z. Yang, H. Wu, X. Chen, and C. Xu, "Hit-Detector: Hierarchical Trinity Architecture Search for Object Detection," in *2020 IEEE/CVF Conference on Computer Vision and Pattern Recognition (CVPR)*. Seattle, WA, USA: IEEE, Jun. 2020, pp. 11402–11411. [Online]. Available: <https://ieeexplore.ieee.org/document/9156291/>
- [16] Y. Sakuma, M. Ishii, and T. Narihira, "DetOFA: Efficient Training of Once-for-All Networks for Object Detection Using Path Filter," Oct. 2023, arXiv:2303.13121 [cs]. [Online]. Available: <http://arxiv.org/abs/2303.13121>
- [17] A. D. Inc., "Adi max78000/max78002 model training and synthesis," <https://github.com/analogdevicesinc/ai8x-training>, 2024, accessed: 2025-10-03.
- [18] Y. Xiong, H. Liu, S. Gupta, B. Akin, G. Bender, Y. Wang, P.-J. Kindermans, M. Tan, V. Singh, and B. Chen, "MobileDets: Searching for Object Detection Architectures for Mobile Accelerators," Mar. 2021, arXiv:2004.14525 [cs]. [Online]. Available: <http://arxiv.org/abs/2004.14525>
- [19] A. Rana and K. K. Kim, "NAS-OD: Neural Architecture Search for Object Detection," in *2024 International Conference on Electronics, Information, and Communication (ICEIC)*, Jan. 2024, pp. 1–3, iSSN: 2767-7699. [Online]. Available: <https://ieeexplore.ieee.org/document/10457265>
- [20] O. T.-C. Chen, Y.-X. Chang, C.-Y. Chung, Y.-Y. Cheng, and M.-H. Ha, "Hardware-aware iterative one-shot neural architecture search with adaptable knowledge distillation for efficient edge computing," *IEEE Access*, pp. 1–1, 2025.
- [21] Y. Sakuma, M. Ishii, and T. Narihira, "Detofa: Efficient training of once-for-all networks for object detection using path filter," in *Proceedings of the IEEE/CVF International Conference on Computer Vision (ICCV) Workshops*, 2023, pp. 1184–1193.
- [22] Y. Kang, B. Zheng, and W. Shen, "Research on oriented object detection in aerial images based on architecture search with decoupled detection heads," *Applied Sciences*, vol. 15, no. 15, 2025.
- [23] Y. Xue, C. Yao, M. Wahib, and M. Gabbouj, "Easfp: Efficient auto-searched feature pyramid for object detection," *Information Sciences*, 2025, preprint or Early Access.
- [24] J. Moosmann, H. Mueller, N. Zimmerman, G. Rutishauser, L. Benini, and M. Magno, "Flexible and Fully Quantized Ultra-Lightweight TinyissimoYOLO for Ultra-Low-Power Edge Systems," Jul. 2023, arXiv:2307.05999 [cs, eess]. [Online]. Available: <http://arxiv.org/abs/2307.05999>
- [25] J. Lin, W.-M. Chen, H. Cai, C. Gan, and S. Han, "MCUNetV2: Memory-Efficient Patch-based Inference for Tiny Deep Learning," Apr. 2024, arXiv:2110.15352 [cs]. [Online]. Available: <http://arxiv.org/abs/2110.15352>